MICROCOPY RESOLUTION TEST CHART

NATIONAL BUREAU OF STANDARDS-1963-A

AD-A183 602

REPORT DOCUMENTATION PAGE

1a REPORT SECURITY CLASSIFICATION (U)	1b RESTRICTIVE MARKINGS NA
2a SECURITY CLASSIFICATION AUTHORITY NA	3 DISTRIBUTION/AVAILABILITY OF REPORT
2b DECLASSIFICATION/DOWNGRADING SCHEDULE NA	Distribution unlimited

DTIC SELECTED AUG 1 1 1987 D

4 PERFORMING ORGANIZATION REPORT NUMBER(S)	5 MONITORING ORGANIZATION REPORT NUMBER(S)

6a NAME OF PERFORMING ORGANIZATION University of Utah	6b OFFICE SYMBOL (If applicable)	7a NAME OF MONITORING ORGANIZATION Office of Naval Research

6c ADDRESS (City, State, and ZIP Code) Salt Lake City, Utah 84112	7b ADDRESS (City, State, and ZIP Code) 800 North Quincy Street Arlington, Virginia 22217-5000

8a NAME OF FUNDING/SPONSORING ORGANIZATION Office of Naval Research	8b OFFICE SYMBOL (If applicable)	9 PROCUREMENT INSTRUMENT IDENTIFICATION NUMBER N 00014-86-K-0230

8c ADDRESS (City, State, and ZIP Code) 800 North Quincy Street Arlington, Virginia 22217-5000	10 SOURCE OF FUNDING NUMBERS			
	PROGRAM ELEMENT NO	PROJECT NO	TASK NO	WORK UNIT ACCESSION NO
	61153N	RR04108	NR or 441	

11 TITLE (Include Security Classification)

Investigation of Resonant AC-DC Magnetic Field Effects

12 PERSONAL AUTHOR(S)
C. H. Durney, J. Janata, A. A. Peterson, A. A. Anderson, C. K. Rushforth

13a TYPE OF REPORT Annual	13b TIME COVERED FROM 5/86 TO 4/87	14 DATE OF REPORT (Year, Month, Day) 1987 July 31	15 PAGE COUNT 36

16 SUPPLEMENTARY NOTATION

17 COSATI CODES			18 SUBJECT TERMS (Continue on reverse if necessary and identify by block number)
FIELD	GROUP	SUB-GROUP	
08			

19 ABSTRACT (Continue on reverse if necessary and identify by block number)

Recently reported observations by others indicates that a combination of a weak dc magnetic field and extra-low-frequency ac magnetic fields can produce resonant effects in biological systems. We have begun a study of resonant magnetic fields that consists of two parts: (1) calculations aimed at identifying the basic mechanisms underlying the resonance, and (2) measurements designed to determine more specifically how biological systems respond to the resonance condition.

We have used a simple model consisting of one charged particle in a viscous medium to explain the basic mechanism of biological resonant response to a combination of dc and ac magnetic fields and ac electric fields. The response is calculated from the Lorentz force equation, which in this case is a system of linear differential equations with time-varying coefficients. Since closed-form solutions are not available, trajectories of the particle are calculated using standard numerical techniques. Conditions for instabilities (unbounded velocity) are calculated from

20 DISTRIBUTION/AVAILABILITY OF ABSTRACT ☒ UNCLASSIFIED/UNLIMITED ☐ SAME AS RPT ☐ DTIC USERS	21 ABSTRACT SECURITY CLASSIFICATION (U)
22a NAME OF RESPONSIBLE INDIVIDUAL Dr. T. C. Rozzell	22b TELEPHONE (Include Area Code) (202) 696-4053	22c OFFICE SYMBOL ONR

DD FORM 1473, 84 MAR   83 APR edition may be used until exhausted   SECURITY CLASSIFICATION OF THIS PAGE
All other editions are obsolete

☆ U.S. Government Printing Office 1986—607-044

19. ABSTRACT

eigenvalues of the system of equations. Numerical values are given for combinations of frequency and magnetic field strengths (resonant conditions) that produce instabilities. Calculated results illustrate both the frequency window and the amplitude window that have been observed by others experimentally. Explanations based on physical interpretation are given for the fundamental mechanisms underlying both phenomena.

We have assembled and tested apparatus for making electrical impedance measurements of planar phospholipid bilayer membranes exposed to combined dc and ac magnetic fields. The impedance is measured with a signal analyzer that is controlled by a microcomputer, which also sets the parameters such as frequency and magnetic fields strength and collects and compiles the data. Preliminary data has been obtained for the plain membrane. We will soon be obtaining data for membranes with channels and other modifications.

Accesion For		
NTIS CRA&I		☑
DTIC TAB		☐
Unannounced		☐
Justification		
By		
Distribution /		
Availability Codes		
Dist	Avail and / or Special	
A-1		

DTIC
COPY
INSPECTED
6

INVESTIGATION OF RESONANT AC-DC MAGNETIC FIELD EFFECTS

Carl H. Durney, Jiri Janata, Arnold A. Peterson, Allen A. Anderson, and Craig K. Rushforth

ABSTRACT

Recently reported observations by others indicates that a combination of a weak dc magnetic field and extra-low-frequency ac magnetic fields can produce resonant effects in biological systems. We have begun a study of resonant magnetic field effects that consists of two parts: (1) calculations aimed at identifying the basic mechanisms underlying the resonance, and (2) measurements designed to determine more specifically how biological systems respond to the resonance condition.

We have used a simple model consisting of one charged particle in a viscous medium to explain the basic mechanism of biological resonant response to a combination of dc and ac magnetic fields and ac electric fields. The response is calculated from the Lorentz force equation, which in this case is a system of linear differential equations with time-varying coefficients. Since closed-form solutions are not available, trajectories of the particle are calculated using standard numerical techniques. Conditions for instabilities (unbounded velocity) are calculated from eigenvalues of the system of equations. Numerical values are given for combinations of frequency and magnetic field strengths (resonant conditions) that produce instabilities. Calculated results illustrate both the frequency window and the amplitude window that have been observed by others experimentally. Explanations based on physical interpretation are given for the fundamental mechanisms underlying both phenomena.

We have assembled and tested apparatus for making electrical impedance measurements of planar phospholipid bilayer membranes exposed to combined dc and ac magnetic fields. The impedance is measured with a signal analyzer that is controlled by a microcomputer, which also sets the parameters such as frequency and magnetic field strength and collects and compiles the data. Preliminary data has been obtained for the plain membrane. We will soon be obtaining data for membranes with channels and other modifications.

1. INTRODUCTION

Much work has been done in the last forty years to determine how electromagnetic fields interact with biological systems. Particularly in the last fifteen years, researchers have exposed hundreds of biological systems to various electromagnetic fields to study their responses. By far the majority of meaningful responses have been attributed to heating of the biological system by the electromagnetic fields. Although there are some responses that are thought to be nonthermal in nature, no one as yet has been able to relate responses to a consistent set of fundamental mechanisms of interaction, and the literature contains inconsistencies and questions about the observations that have been made. Perhaps this is not surprising in view of the great complexity of biological systems and

the tremendous number of combinations of parameters that could be included in an experiment. For example, the frequency of the electromagnetic fields could vary over the spectrum from dc to 300 GHz. Couple this with the many possible combinations of electric and magnetic field strengths and configurations, and the number of experimental parameters is unmanageably large. Add to this the huge humber of biological systems that could be studied, all the way from the simplest in-vitro preparation to the complex behavioral patterns of whole organisms, and the matrix of possible experimental parameters is overwhelming.

In view of all this complexity, some recent observations are particularly intriguing for two reasons: first, they appear to indicate an effect that is perhaps more robust than many other observations, and second, they may be more readily explainable in terms of basic physical principles than most other observations. These recent observations are biological responses to combinations of dc and ac magnetic fields, apparently in some kind of a resonance reaction. Although dc magnetic fields, particularly that of the earth, have not usually been considered important in experiments involving electromagnetic radiation of biological systems, several recent publications may indicate a common underlying magnetic field resonance effect produced by combinations of dc and ac magnetic fields.

Jafry-Asl et al. [1983] report a resonance effect on the dielectrophoretic yield in in-vitro preparations of yeast cells. They also found a resonance effect on the permittiv. ty of the yeast cells. Their proposed explanation is a nuclear magnetic resonance (NMR) effect produced by the earth's magnetic field, but this may not be likely for several reasons. First, a NMR effect would be expected to be negligible in their dc magnetic field of less than a hundred microtesla because the energy of a magnetic dipole in that field would be something like nine orders of magnitude smaller than kT, which means that the applied magnetic fields would have a very small effect compared to the thermal excitation. Secondly, in their dielectrophoretic cell, only an ac electric field was applied. The NMR effect requires an ac magnetic field. There would, of course, be an ac magnetic field accompanying the applied ac electric field in their cell, but it would be negligibly small at those low frequencies (less than a few kHz).

Delgado et al [1982] and Ubeda et al [1983] exposed fertilized chicken eggs to pulsed magnetic fields and found strong developmental effects at field strengths of 1.2 microtesla and 12 microtesla when the pulse width was 0.5 ms and the repetition rates were 100 Hz and 1000 Hz. Although they did not give the information in their original published articles, the authors have stated in discussions that the effects did not occur unless the eggs were oriented east-west, which in their configuration meant that the applied ac magnetic field was perpendicular to the earth's magnetic field. The authors did not propose a mechanism of interaction, and they did not mention the possibility of a magnetic-field resonance effect, but the fact that the orientation of the eggs in the earth's magnetic field is crucial indicates that a magnetic field resonance effect could have occurred. According to news reports [Microwave News, 1984], two investigators in the United States have not been able to

2

reproduce the results of Delgado and his colleagues, but a researcher in Sweden has. The effects found by the Swedish worker were, however, not as strong as those found by Delgado et al. Since the U. S. investigators did not report having tried to duplicate the dc magnetic field values of the Delgado laboratory, it may be possible that their failure to replicate the work was caused by a different ac-dc magnetic field combination.

In other work that depends upon dc-ac magnetic fields, Blackman et al [1985] found that changes in calcium efflux occurred in chick-brain preparations only if the frequency of the applied ac fields was properly related to the dc magnetic field that was present. The authors suggested some sort of cyclotron resonance as the explanation for the required combination of dc-ac magnetic fields. This recent data showing the dependence of the change of calcium efflux on the dc magnetic field may possibly explain why others have not been able to replicate the data of Blackman et al, since apparently no one expected the dc magnetic field to be an important parameter.

More recently, Thomas et al [1986] have shown a strong behavioral effect in rats exposed to combined dc-ac magnetic fields. These investigators sudied the effects of 60 Hz electric and magnetic fields on the abilities of rats to press levers within a narrow time window after a stimulus. They had found no significant effects in their previous studies in a laboratory ambient dc magnetic field of about 40 microtesla. However, when they adjusted the dc magnetic field to 26 microtesla, they found a significant effect on the rats' abilities to time the lever pressing. According to the authors, they chose the 26 microtesla field to correspond to the cyclotron resonance of a bare lithium ion at 60 Hz. Although the mechanism for this effect has not yet been identified, the effect is certainly a striking indication of the biological effects of magnetic field resonance.

McLeod and Liboff [1986] showed that the motility of a diatom preparation on a calcium impregnated agar substrate was highly dependent on the calcium concentration. Then they exposed the diatom preparation to the combination of a parallel dc and ac magnetic field and showed that the motility showed a strong resonance with frequency, centered about the cyclotron resonance frequency of a bare calcium ion. The resonance frequency was directly proportional to the dc magnetic field strength. These experiments are strong evidence of a biological response that is clearly related to resonant dc-ac magnetic field conditions.

There are a number of other reports of low-frequency magnetic fields causing significant biological responses, but with no mention of the possible role of the ambient dc magnetic field that is always present unless it is deliberately cancelled or shielded against. Since the dc magnetic fields required for the resonant effects described above are of the same order as a typical laboratory ambient magnetic field (the 26 microtesla used by Thomas et al [1986], for example), the laboratory ambient magnetic field could have played an unobserved role in many experiments. For example, Conti et al [1983, 1985] report that 3 Hz magnetic fields with intensities of 2.3-6.5 millitesla reduced the mitotic stimulation of human lymphocytes, and reduced the Ca^{2+} uptake by stimulated lymphocytes. It is conceivable that the frequency window they found within which ConA-induced blastogensis was

3

reduced by magnetic fields is due to a resonance with the dc magnetic field. This is only speculation, but since Blackman et al [1984] found that the dc magnetic field resonance signficantly affected their measurement of calcium efflux, it is not entirely improbable.

Although cyclotron resonance for electrons in free space is familiar, few theoretical studies of effects of ac-dc magnetic fields on biological systems have been conducted. Chiabrera et al [1985] made calculations for a model of a charged ligand in the microenvironment of its binding site, which demonstrated a cyclotron-type resonance. Liboff [1985] made some calculations of cyclotron frequencies for ion species, and Mc Cleod and Liboff [1986] calculated the response of ions to ac-dc magnetic fields, but their calculations do not include the ac magnetic field, except in a very limited approximation.

The purpose of this project is to explore basic mechanisms that might be involved in biological responses to resonant dc-ac magnetic fields such as those described above. We have made calculations for a simple model to explain the basic mechanisms that underlie the resonance response and to guide our experimental work. On the experimental side, we have assembled and tested apparatus for measuring the electrical impedance of phospholipid bilayer membranes exposed to combined dc and ac magnetic fields. In this report, the modeling and calculations are described first, followed by a description of our experimental work.

2. MODELING AND CALCULATIONS

Since biological systems are extremely complex, any models that might describe the basic resonance interactions will be very complicated. In searching for basic mechanisms of interaction in such complicated systems, we believe it fruitful to begin with the simplest model that may describe the interaction, learn from it the fundamental characteristics of the interaction, and then improve the model and develop more complex analyses. In line with that reasoning, we have studied a very simple model consisting of a single charged particle in a viscous medium exposed to a combination dc-ac magnetic field. The magnetic fields are uniform in space with an arbitrary angle between their direction (the equations are derived for an arbitrary angle, but the first calculated data is for parallel magnetic fields). We included the ac electric field induced by the ac magnetic field, assuming cylindrical or spherical geometry, such as might exist in a single dielectric sphere that could be viewed as a crude model of a biological cell. The viscous medium is represented in the Lorentz force equation by a damping term that is proportional to velocity. We solved the Lorentz force equation to obtain the motion of the charged particle in the viscous medium. Although this model is very crude compared to any biological system, we believe it is a valid and indeed appropriate first step in understanding biological responses to resonant dc-ac magnetic fields because whatever effect the magnetic fields have on the biological system is through the forces exerted by the magnetic fields on charged particles in the biological system. Thus the response of one charged particle to the forces of the magnetic fields can perhaps give insight about how the biological system might be affected by the resonant magnetic

fields. This insight could prove to be invaluable in analyzing more complicated models and in designing experiments.

In this section we first describe the model and equations of motion of the charged particle. Then we discuss qualitatively the response of a charged particle to various simple electromagnetic field configurations. Next we discuss the differential equations of motion, their characteristics and methods of solution. Finally, we show calculated responses of a charged particle to resonant magnetic fields and discuss the meaning of these results.

2.1 Model

The model consists of one charged particle in a viscous medium exposed to a dc magnetic field, an ac magnetic field, and an ac electric field induced by the ac magnetic field, as shown schematically in Fig. 1. This model does not represent a biological system, which is obviously much more complex than one charge in a viscous medium. The purpose of the model is to identify basic concepts and fundamental mechanisms of interaction involved in resonance response, to provide physical interpretation and qualitative understanding. The information obtained from this simple model might then be used as a basis for formulating realistic models of biological systems.

The Lorentz force equation describes the effect of the fields and the viscous medium on the particle. Each of the elements of the model is described in detail below.
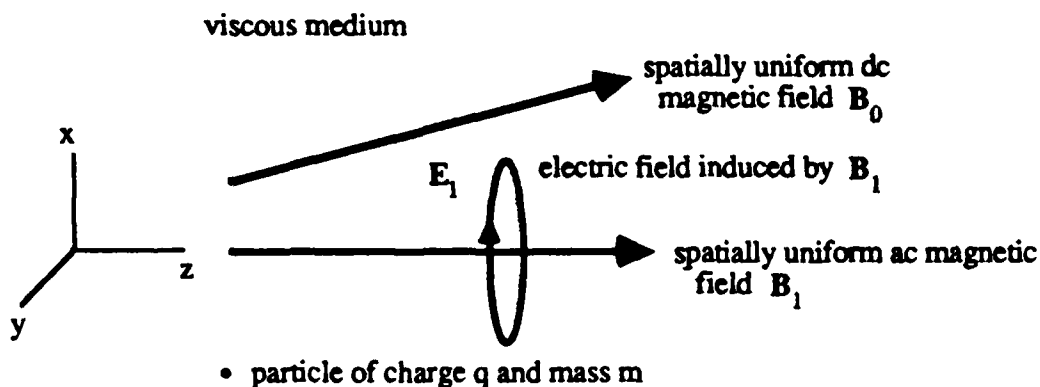

Fig. 1. Model consisting of a single charged particle in a viscous medium exposed to electric and magnetic fields. The magnetic fields are uniform in space; the electric field is not.

2.1.1 Electromagnetic Fields. In this model, the dc and ac magnetic fields are both uniform in space. We have used "ac" to indicate that the magnetic field is time varying, but not necessarily sinusoidally. (The calculated data in this report is for sinusoidal time variation, but the equations are derived for general time variation.) An expression for the E field induced by the time-varying magnetic field can

be easily derived from Maxwell's equation when cylindrical or spherical symmetry is present, as follows. Maxwell's curl E equation in integral form is

$$\int \mathbf{E}_1 \cdot d\mathbf{l} = -\int \frac{\partial \mathbf{B}_1}{\partial t} \cdot d\mathbf{S} \tag{1}$$

Assuming that $\mathbf{B}_1$ is in the z direction and from symmetry that E has only a ϕ component that varies only with r, either in cylindrical or spherical coordinates, allows (1) to be integrated to get

$$2 \pi r E_\phi = -\frac{\partial B_1}{\partial t} r^2$$

where bold-face symbols indicate vector quantities and plain symbols indicate scalars and magnitudes of vector quantities. Solving for E_ϕ and transforming to rectangular coordinates gives

$$\mathbf{E}_1 = \frac{1}{2} (y \mathbf{x} - x \mathbf{y}) \frac{\partial B_1}{\partial t} \tag{2}$$

where x and y are unit vectors in the x and y directions, respectively.

Equation (2) represents the E field induced by $\mathbf{B}_1$ in any geometry that has cylindrical or spherical symmetry. This would apply to the configuration shown in Fig. 2, for example, which is a dielectric sphere in a conducting medium.

An important characteristic of the electromagnetic fields of this model is that the externally applied $\mathbf{B}_1$ will penetrate a highly conducting medium and induce in that medium the electric field given by (2). In contrast, an externally applied electric field would tend to be shorted out by the conducting medium and would be quite different in nature from (2). This model may describe, therefore, a mechanism whereby an externally applied magnetic field could have more effect on internal charges in a highly conducting medium than an externally applied electric field.
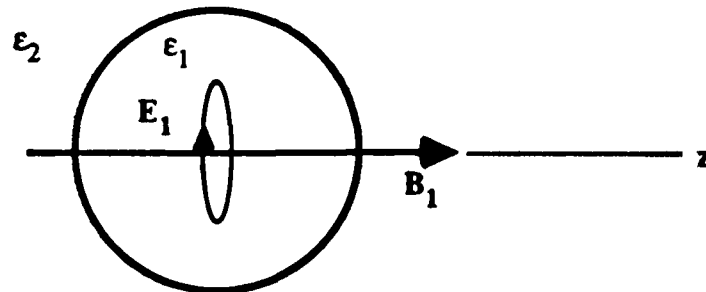
Fig. 2. A sphere of complex permittivity ε_1 in a medium of complex permittivity ε_2 and the E field (given by (2)) induced by the time-varying magnetic field B_1.

2.1.2 Equations of Motion. The basic equation that describes the motion of the charged particle (Fig. 1) in the presence of the electromagnetic fields is

$$m\frac{dv}{dt} + m \nu v = q E + q v \times B \tag{3}$$

where the first term is the inertial force term, the second is the force due to drag in the viscous medium, and the terms on the right-hand side are the forces produced by the electric and magnetic fields, respectively. Since (3) is a vector differential equation that includes a cross product, it is rather complex. With the geometry as defined in Fig. 1, (3) can be written as three simultaneous scalar differential equations:

$$x'' + \nu x' = \eta E_x + \frac{\omega_{c1}}{2} h' y + \omega_{c1} h y' + \omega_{cz} y' - \omega_{cy} z' \tag{4}$$

$$y'' + \nu y' = \eta E_y - \frac{\omega_{c1}}{2} h' x - \omega_{c1} h x' + \omega_{cx} z' - \omega_{cz} x' \tag{5}$$

$$z'' + \nu z' = \eta E_z + \omega_{cy} x' - \omega_{cx} y' \tag{6}$$

where the following definitions have been made:

(x,y,z) is the position of the particle at time t

$x' = dx/dt$, etc.

E_x, E_y, E_z, are the applied electric field

$$B_1 = B_1 h(t) z \tag{7}$$

$$B_0 = B_{0x} x + B_{0y} y + B_{0z} z \tag{8}$$

$$\omega_{c1} = q B_1/m \tag{9}$$

$$\omega_{cx} = q B_{0x}/m, \text{ etc.} \tag{10}$$

$$\eta = q/m \tag{11}$$

Equations (12) and (13) are similar in form to those derived by Chiabrera et al (1985) for a more sophisticated model that includes a collection of charged particles and describes ligand binding. After they made some simplifying assumptions, their differential equations reduced to a form similar to (12) and (13), but their induced electric field is constant in space, in contrast to the variation with x and y described in (2).

We have included an externally applied electric field in (4) - (6) for generality, but we will mostly be interested in the case where there is only an E field induced by B_1. For the special case

7

when there is no externally applied electric field and the dc magnetic field is in the z direction, (4) - (6) reduce to the following two simultaneous equations in x and y:

$$x'' + v\,x' - \frac{\omega_{c1}}{2}\,h'\,y - (\omega_{c1}\,h + \omega_c)\,y' = 0 \qquad (12)$$

$$y'' + v\,y' + \frac{\omega_{c1}}{2}\,h'\,x + (\omega_{c1}\,h + \omega_c)\,x' = 0 \qquad (13)$$

where $\omega_c = q\,B_0/m$. These equations are linear homogeneous differential equations with time varying coefficients. Since they are homogeneous, x and y can be normalized to any convenient quantities, such as the beginning resting position of the particle or the diameter of a biological cell. When h(t) is a sinusoidal steady-state function, t can be normalized to T, the period of the sinusoid, which also allows v to be normalized to f, where $f = 1/T$, and ω_c and ω_{c1} to be normalized to ω, where $\omega = 2\pi/T$ This provides a very convenient way to calculate and display the responses of the charged particle to the driving fields. Methods for solving the differential equations are discussed in the next section.

2.2 Solution of the Equations of Motion

The equations of motion are linear differential equations with time-varying coefficients. For all the cases of interest here, the time-varying coefficients will usually be periodic because the ac magnetic field will be periodic. With periodic coefficients, the equations can be transformed into an equation known as Hill's equation [Reinhard, 1987]. Although Floquet's theorem can be used to show that periodic solutions to these equations exist, no closed-form solution is available. Much has been written about the solution to Hill's equation and other equations with periodic time-varying coefficients, but it appears that no method of solution is available except the usual numerical methods for solving differential equations. We have, however, developed methods for determining regions of instability. We describe these next, and then discuss the numerical solution of the differential equations with periodic time-varying coefficients.

2.2.1 Calculation of Instability Criteria.

In this section we consider a special case of equations (12) and (13) obtained by setting $h(t) = \sin \omega t$. We further define the state variables

$$x_1(t) = x'(t)$$
$$x_2(t) = x(t)$$
$$x_3(t) = y'(t)$$
$$x_4(t) = y(t)$$

and write (12) and (13) as the system of first-order equations

8

$$x'(t) = A(t) x(t) \tag{14}$$

where $x^T = (x_1, x_2, x_3, x_4)$ and

$$A = \begin{bmatrix} -\nu & 0 & (\omega_{c1}h + \omega_c) & \omega_{c1}h'/2 \\ 1 & 0 & 0 & 0 \\ -(\omega_{c1}h + \omega_c) & -\omega_{c1}h'/2 & -\nu & 0 \\ 0 & 0 & 1 & 0 \end{bmatrix} \tag{15}$$

Systems of linear ordinary differential equations with periodic coefficients, of which (14) is an example, are frequently encountered in modeling physical systems and have been extensively studied. Our purpose in this section is to investigate the stability of (14) as the parameters are varied. We begin with a definition.

The **resolvent** $\emptyset(t,s)$ associated with (14) is the unique matrix satisfying

a. $\emptyset(t,t) = I$ for all t.
b. $\emptyset(t,s) = \emptyset(t,u) \emptyset(u,s)$ for all s, t, u.
c. $\partial \emptyset(t,s)/\partial t = A(t) \emptyset(t,s)$
d. $\partial \emptyset(t,s)/\partial s = -\emptyset(t,s) A(s)$

As the followi..g theorem shows [Reinhard, 1987], the resolvent plays a fundamental role in determining the stability of (14).

Consider (14) under the assumption that A(t) is periodic with period T.

a. The system described by (14) is uniformly asymptotically stable if and only if all the eigenvalues of $\emptyset(T,0)$ have magnitudes strictly less than 1.
b. The system described by (14) is uniformly stable if and only if all eigenvalues of $\emptyset(T,0)$ are less than or equal to 1, with all eigenvalues of magnitude 1 having index 1.
c. In all other cases, the system described by (14) is unstable.

In view of this theorem and the preceding definition, we arrive at the following procedure for determining the stability of (14):

1. Select values for the parameters

9

2. Solve the equation $\emptyset'(t,0) = A(t)\,\emptyset(t,0)$ on the interval $[0,T]$ with initial condition $\emptyset(0,0) = I$.

3. Calculate the eigenvalues of $\emptyset(T,0)$.

4. If any eigenvalue has magnitude greater than 1, or if any eigenvalue with magnitude 1 has index greater than 1, the system is unstable.

In terms of our model, instability means that the displacement and velocity of the charged particle would increase without bound as t increases. We cannot solve the equation in step 2 analytically, and therefore must rely on numerical methods. We solved this equation for a wide range of parameter values using a numerical routine developed by Shampine and Gordon [1975], and the predicted conditions for instability agree with results of the numerical calculations described in the next section. Since this technique allows us to determine whether the system is unstable for a given combination of parameters, it is an important complement to the numerical solutions, which cannot predict instabilities as such, but can only give indications of possible instabilities. The numerical solutions, on the other hand, can give other useful information and much insight about the response of the system. The combination of the two methods is a powerful tool for investigating the response of a charged particle to the EM fields.

2.2.2 Numerical Solution. To explore the nature of the response of a charged particle to the fields of our model, we have solved (12) and (13) by several methods and compared results to ensure the validity of the solutions. These methods include the numerical routine developed by Shampine and Gordon [1975] a Runge-Kutta routine, a predictor-corrector method, and a power series solution. The solutions obtained by all these methods have been consistent and numerically very close to each other, indicating that we have valid solutions.

2.2.3 Numerical Determination of Resonance Conditions. To check the instability predictions described in the section on solution of the equations of motion, we made some additional numerical calculations using the following steps:

1. The particle is assumed to be initially at rest.

2. The position of the particle is calculated as a function of time for various combinations of ω, ω_{c1}, and ω_c for a total time equal to a specified number of periods of ω. Thus for lower frequencies, the calculations were made for a longer time.

3. The maximum distance of the particle from its resting point at any instant during that total time was recorded and plotted.

The resulting calculated maximum displacements are consistent with the predicted instabilities, which show strong resonance behaviors. Before describing the results of the instability calculations in

10

a later section, we discuss the general qualitative nature of the response of charged particles to combined dc-ac electromagnetic fields next.

2.3 Response to Resonant Electromagnetic Fields

In this section, we describe in qualitative terms the response of a charged particle to some specific combinations of electric and magnetic fields to illustrate the basic characteristics of such response, in particular, the nature of resonance response.

2.3.1 Response to E Alone. The response of a charged particle initially at rest at the origin of a coordinate system to an ac electric field alone is shown in Fig. 3. Since the forces on the particle always lie along the direction of E, the particle retraces the same path, oscillating in direction with E. This response results in no net charge transport, since the particle merely oscillates about a point midway between its initial resting point and its maximum excursion from that initial point.
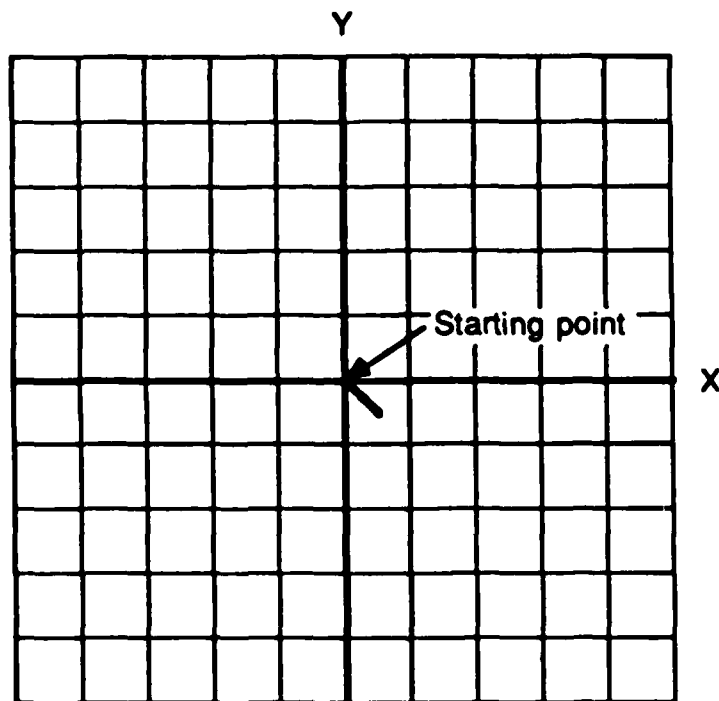
Fig. 3. Response of a charged particle at the origin to a spatially uniform ac E field with no magnetic fields present. The direction of E is at 45 degrees to the x axis in the fourth quadrant. The particle continuously retraces the path shown.

2.3.2 Response to E and B_0. Figure 4 shows the significant difference in response when a static magnetic field is added to the E field of Fig. 3. The addition of the $v \times B$ force in (3), which is always perpendicular to both v and B, causes the particle to travel in a spiral path perpendicular to the B field.

In contrast to the response in Fig. 3, this resonant response could result in a net transport of charge because the particle would not return to its starting position. This spiral path results at resonance, that is the ac frequency of the electric field is equal to the cyclotron frequency of the charged particle, as defined by (10). When this condition is met, the reversal of the forces due to the change in direction of E as it oscillates always occurs at just the right time in the orbit of the particle to enhance its motion along the spiral path. When this condition is not met, the reversal in the forces due to E will tend to oppose the particle's motion, and the velocity of the particle will therefore not build up. This nonresonant response is illustrated in Fig. 5.
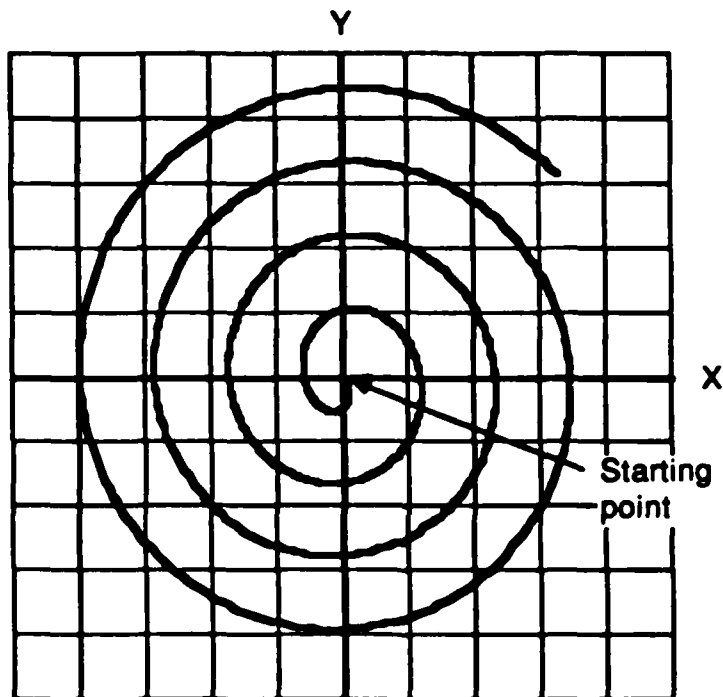
Fig. 4. Response of a charged particle initially at rest at the origin in the presence of the same E field as in Fig. 3 and a spatially uniform static magnetic field in the z direction. $\omega = \omega_c = 62.8$ radians/sec, where ω is the frequency of E and ω_c is the cyclotron frequency (see (10)), and $v = 0$ (no viscous damping). The position of the particle is plotted for four complete cycles of E.
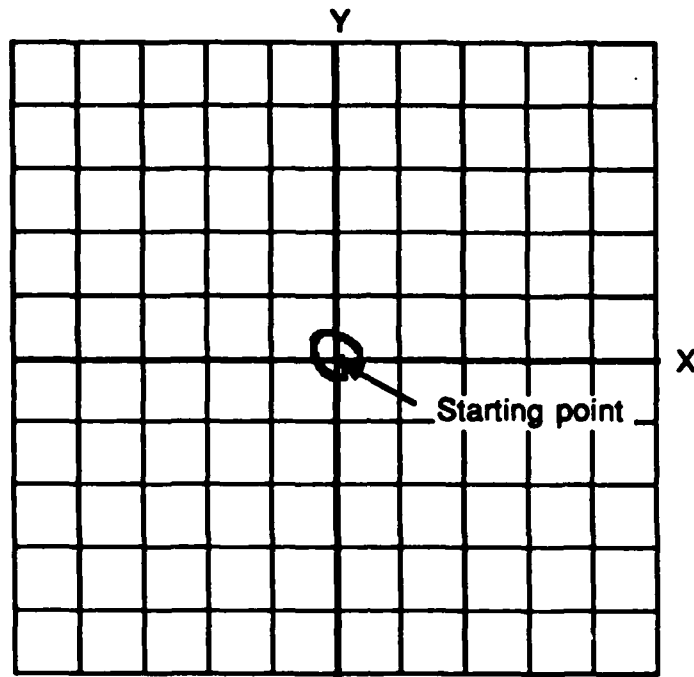
Fig. 5. Response for the same conditions as in Fig. 4, except $\omega = 2\omega_c$.

The effect of viscous damping is shown in Fig. 6. With viscous damping respresented by a collision frequency of 25 Hz, the motion of the particle for four cycles of E is highly damped, as compared with the response without damping in Fig. 4.
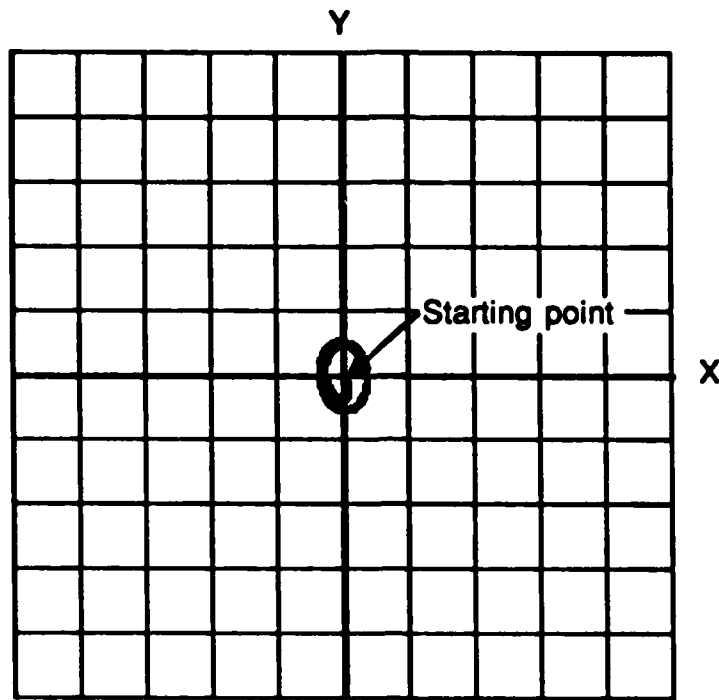
Fig. 6. Response of the charged particle for the same conditions as Fig. 4 except that $v = 25$ Hz.

The nature of the E field has a signficant effect on the path of the particle. Fig. 7 shows the response to an E of the form of (2), that is E is in the ϕ direction and proportional in magnitude to distance from the origin, but there is no ac magnetic field in the v x B term. The electric field strength also has a large effect on the nature of the particle path.
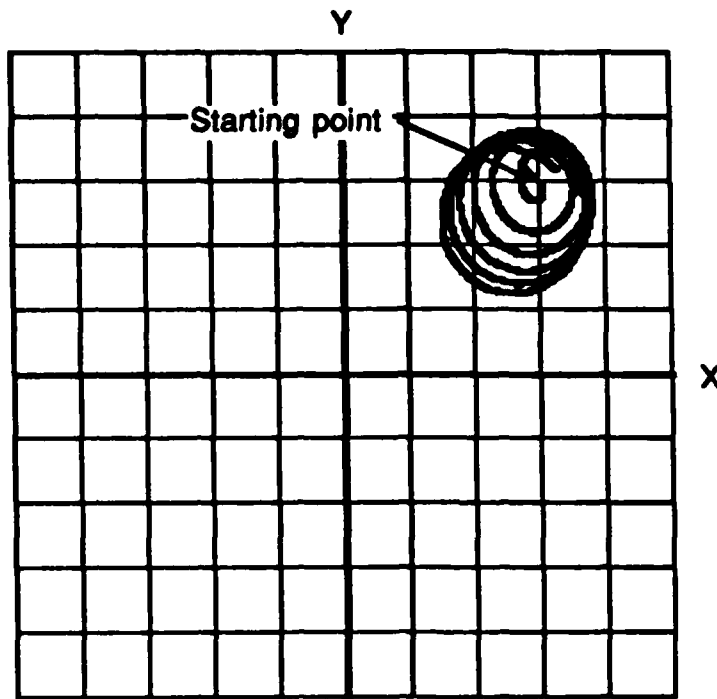
Fig. 7. Response to E and B_0, where E is of the form given by (2), that is, E is in the ϕ direction with a magnitude proportional to distance from the origin, but there is no ac magnetic field in the $v \times B$ term. $\omega = \omega_c = 628$ radians/sec, $\omega_{c1} = 62.8$ radians/sec, $v = 50$ Hz.

2.3.3 Response to E, B_0, and B_1. Adding the ac magnetic field in the $v \times B$ term complicates the nature of the forces and the resulting response. Figure 8 shows the particle response to the same parameters as in Fig. 7, but with the ac magnetic field force added. For this particular set of parameters, the displacement in the radial direction is opposite from that of Fig. 7. In Fig. 8 and all succeeding figures that represent the solution to (12) and (13), X and Y can be considered normalized to the coordinates of the initial position of the particle, as described in Section 2.1.2. This is possible because every term in (12) and (13) contains an x or y. Thus in Fig. 8 if each unit on the axes represents 25 microns, the particle would have started at 75 microns on the x axis and 75 microns on the y axis, and the subsequent displacement represented in the figure would also be given in microns as indicated by the position with respect to the coordinate system.
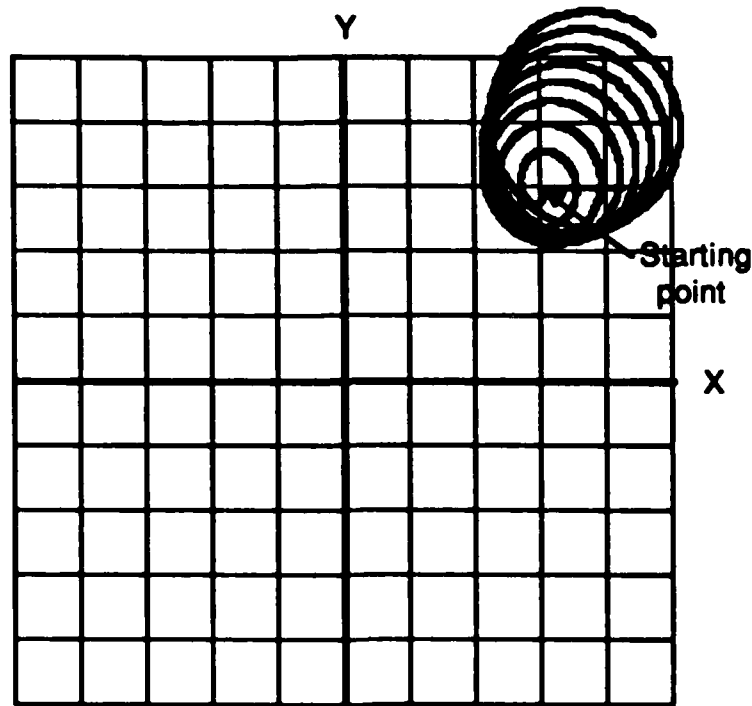
Fig. 8. Response of a charged particle to combined ac and dc magnetic fields, with the E field induced by the ac magnetic field, as described by (2). $\omega = \omega_c = 628$ radians/sec, $\omega_{c1} = 62.8$ radians/sec, $\nu = 50$ Hz. The X and Y are normalized to the starting position of the particle.

Figure 9 shows the striking effect of resonance on the response of the particle. The parameters are the same as for Fig. 8, except ω_{c1} has been increased to be equal to ω and ω_c. Because the response was so much greater, the scale has been changed by a factor of 10 in Fig. 9 compared to Fig. 8 so the path could be shown on one sheet. Thus if one unit on the axes in Fig. 8 represents 25 microns, one unit on the axes in Fig. 9 represents 250 microns. The resulting greater displacement of the particle from its initial position of rest shows how great the effect of resonance can be.
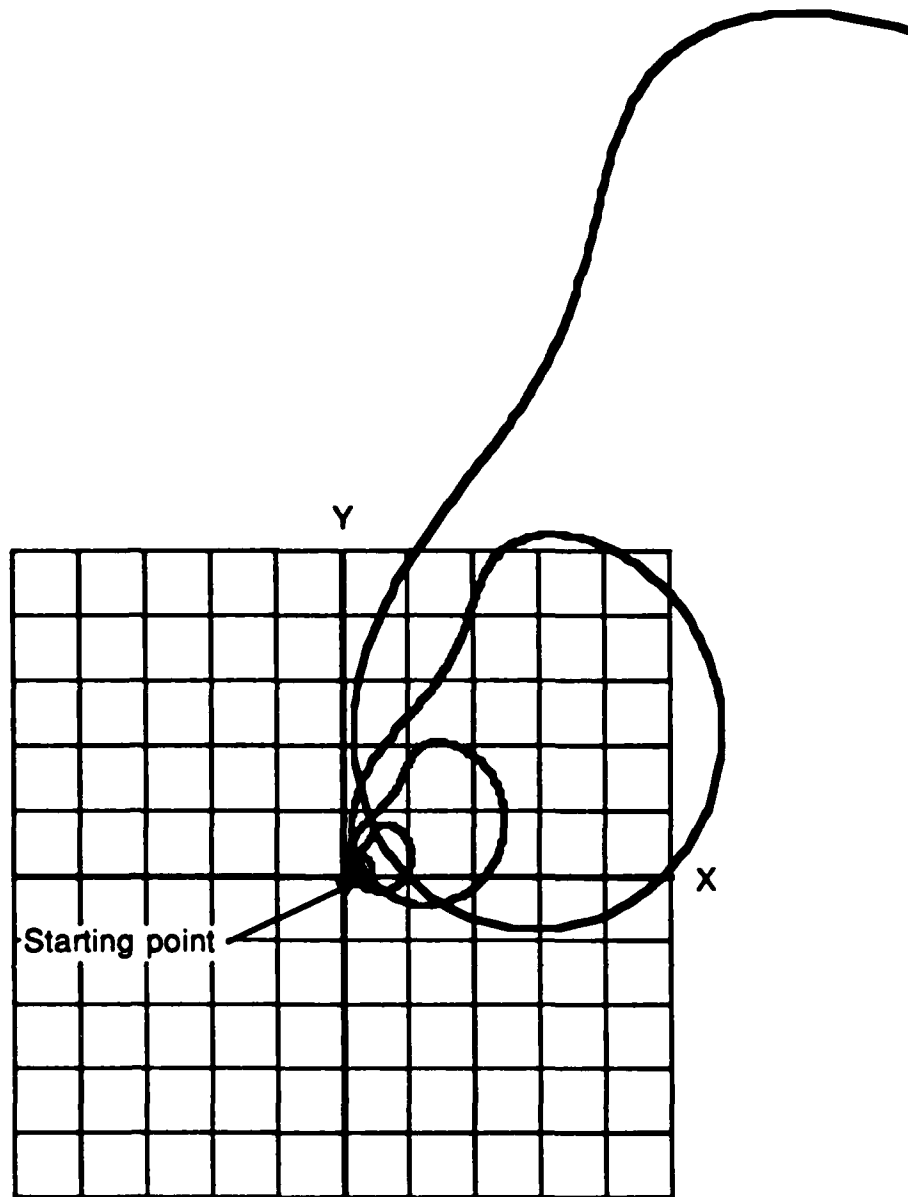
Fig. 9. Response for the same parameters as in Fig. 8 except ω_{c1} = 628 radians/sec. The scale here is tenfold different from that in Fig. 8. For example, if one unit on the axes in Fig. 8 represents 25 microns, one unit here represents 250 microns.

The dramatic effect that the amplitude of the ac magnetic field can have on the response is shown in Fig. 10, which is the response for the same set of parameters as in Fig. 9, except ω_{c1} = 1200. Even though the ac field strength is considerably higher in Fig. 10, resulting in a much stronger E and therefore stronger forces, the displacement of the particle from the origin is generally much less. This is like the "amplitude window" (or power-density window) observed experimentally in the calcium efflux experiments [e.g., Bawin and Adey, 1976; Blackman et al, 1982].
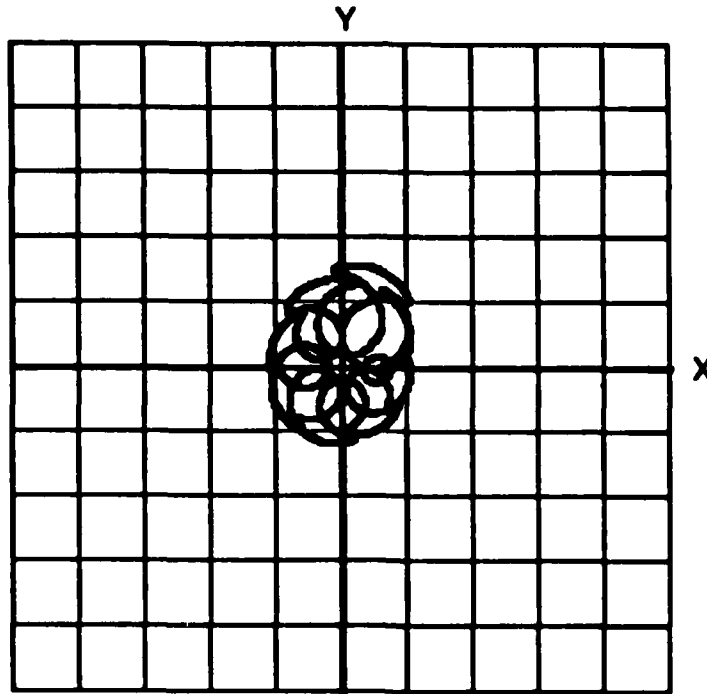
17

Fig. 10. Response for the same parameters as in Fig. 8, except $\omega_{c1} = 1200$. The scale is the same as in Fig. 8, which means it differs by a factor of ten from that in Fig. 9.

Figure 11 shows another example of how sensitive the response is to the combination of parameters. Here $\omega = \omega_c = \omega_{c1}$, but they are all lower in value than in Fig. 9. The response here is not nearly as great as it is in Fig. 9. One reason may be that the ratio of the collision frequency to the ac frequency in Fig. 11 is larger than it is in Fig. 9. It appears that the magnitude of the resonance response becomes smaller as the ratio of the collision frequency to the ac frequency becomes larger.
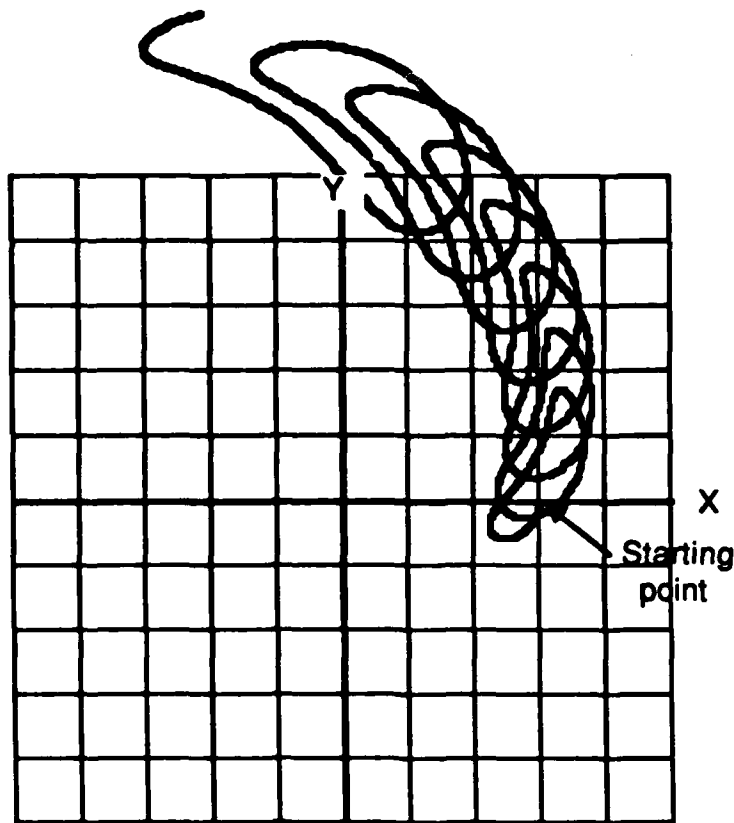
Fig. 11. Response for the same parameters as in Fig. 8 except $\omega = \omega_c = 62.8$ radians/sec.

2.4 Conditions for Resonance

Using the techniques described in the Section 2.2, we calculated the eigenvalues that describe the instabilities of the response for a wide range of the parameters ω, ω_{c1}, v, and ω_c. As explained previously, we normalized the differential equations to T, the period of the ac magnetic field, which allowed normalization of all frequencies to ω. The instability data are presented as a function of ω_{cn} = ω_c /ω, $\omega_{c1n} = \omega_{c1}/\omega$ and $v_n = v/f$, where $\omega = 2\pi f$.

Figure 12 shows a plot of the eigenvalues on a grid of ω_{c1n} and ω_{cn} for $v_n = 0$. The plane where the eigenvalues are equal to unity is clearly evident in the lower right-hand part of the plot. The larger the eigenvalue, the faster the velocity and displacement of the particle from its rest position increases. Thus the eigenvalue peaks indicate the conditions for greatest instability. The peaks do not appear smooth because the grid on which the calculated values were obtained was not fine enough; a finer grid would require more computer time. Figure 13 shows how the eigenvalues are modified by increasing the collision frequency v. Figure 14 shows the plots for a finer mesh, and Figs. 15 and 16 show the effect of increasing the collision frequency. It is clear that for this model no resonance response could occur when the collision frequency is signficantly higher than the frequency of the applied fields.

19

Figures 17 and 18 show contour plots of the eigenvalues, which are like looking down on the plots of Figs. 12 and 13. Only the contours for eigenvalues greater than unity are shown. These contour plots make it easier to determine the combinations of ω_{c1n} and ω_{cn} that produce instabilities. For example, from Fig. 17, it can be seen that one peak in eigenvalues occurs when $\omega_{cn} = 0.75$ and $\omega_{c1n} = 1.25$. Thus for any ω for which the electric and magnetic fields are those of the model, instabilities are predicted for the conditions $\omega_{cn} = 0.75$ and $\omega_{c1n} = 1.25$. Other peaks are located in a nearly periodic set of positions.

It is important to remember that the conditions for resonance as shown in Figs. 17 and 18 apply only to the model used here, in which the ac and dc magnetic fields are parallel, and there is no externally applied electric field. Different contour plots would be expected for other field configurations. For example, if an external electric field were applied, resonant conditions along the $\omega_{c1n} = 0$ axis would be expected. There are no resonances for $\omega_{c1} = 0$ in our model because that condition means no ac electric field is present, which means that a particle at rest would remain at rest. Also, other components of ac and dc magnetic fields might produce other resonances. Furthermore, electric and magnetic fields with waveforms different from sinusoids would be expected to produce different resonance conditions. We are presently extending our calculations to include other waveforms, but only results for sinusoids are given in this paper.

Some interesting observations can be made from Figs. 17 and 18. First, a comparison of Figs. 17 and 18 seems to indicate that the position of the peaks are not affected much by the collision frequency. A more detailed study of the effects of the collision frequency shows that indeed the positions of the peaks are not affected much by the value of v, but the magnitude of the peaks is signficantly affected by v. Second, resonances can occur even when there is no dc magnetic field present, that is, when $\omega_{cn} = 0$. These resonances occur only for specific values of ω_{c1n}, again indicating the presence of an amplitude widow. A third observation is that the linewidth of the resonance does not seem to be affected much by the value of v. It might have been reasonable to expect from experience with other resonant systems that when the damping went to zero, the linewidth would also go to zero. Figure 17 indicates that this is surely not the case.

All of these observations are explained in terms of physical concepts of the interaction between the charged particle and the applied electromagnetic fields in the following section.
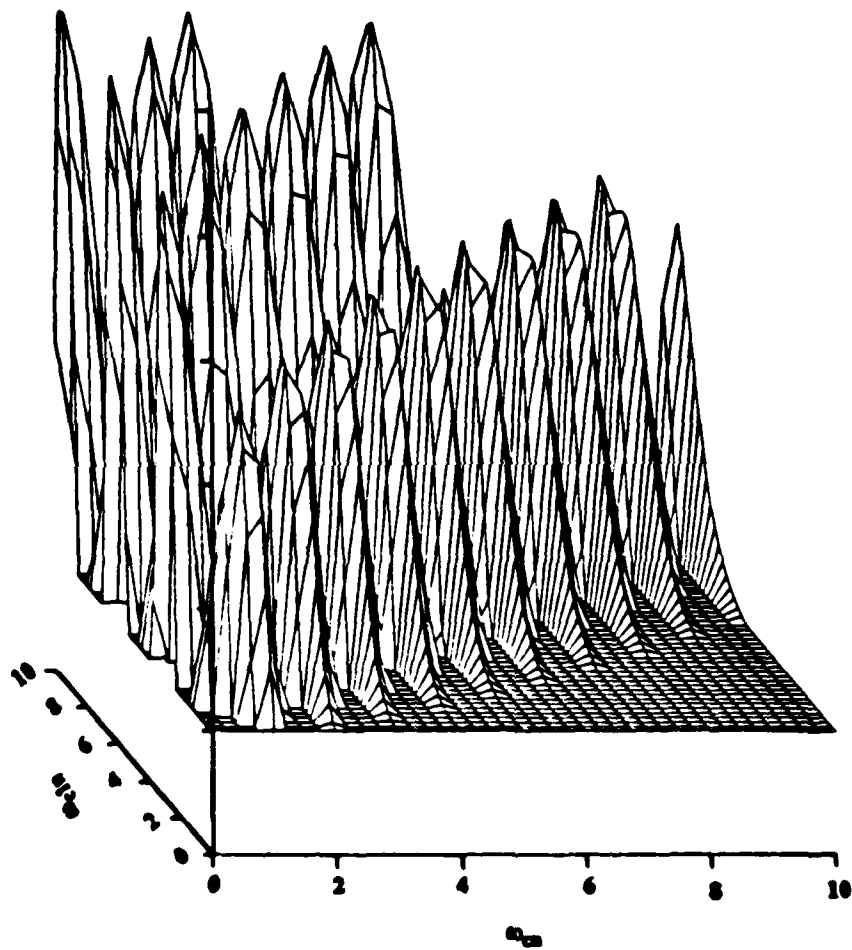
Fig. 12. Magnitude of the eigenvalues as a function of $\omega_{cn} = \omega_c/\omega$ and $\omega_{c1n} = \omega_{c1}/\omega$ for $\nu_n = 2\pi\nu/\omega = 0$. Each division on the vertical axis equals 1 unit.

21

Fig. 13. Magnitude of the eigenvalues as a function of $\omega_{cn} = \omega_c/\omega$ and $\omega_{c1n} = \omega_{c1}/\omega$ for $v_n = 2\pi v/\omega = 1$. Each division on the vertical axis equals 0.5 units.

Fig. 14. Magnitude of the eigenvalues as a function of $\omega_{cn} = \omega_c/\omega$ and $\omega_{c1n} = \omega_{c1}/\omega$ for $\nu_n = 2\pi\nu/\omega = 1$. Each division on the vertical axis equals 0.5 units.
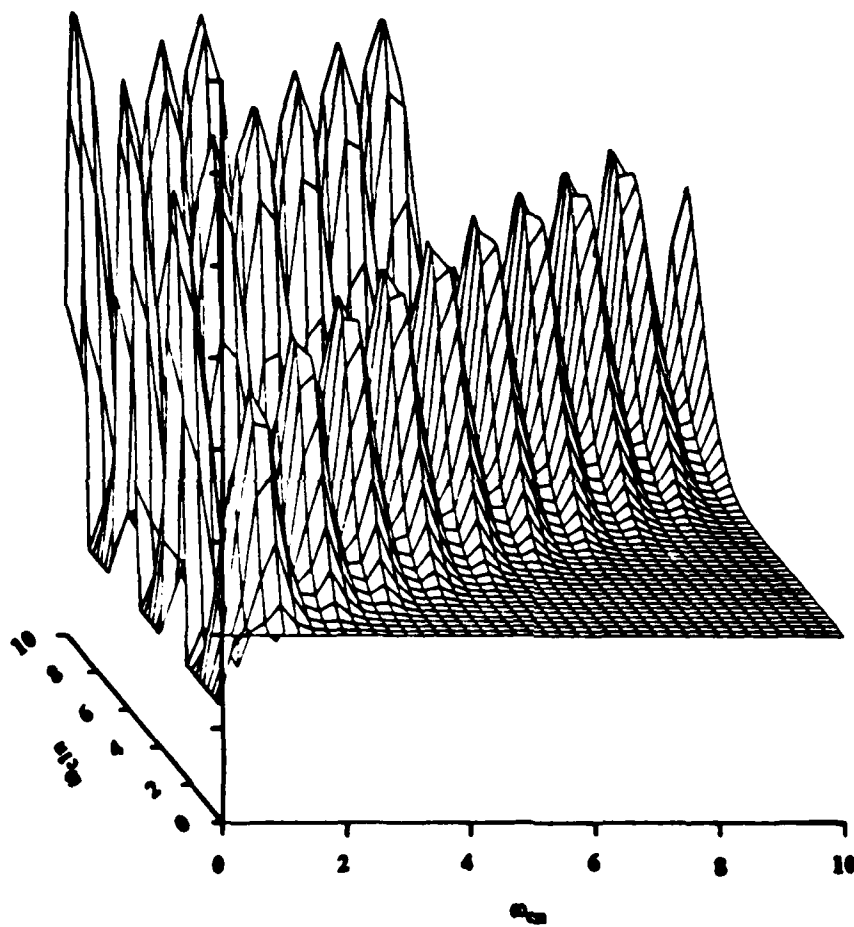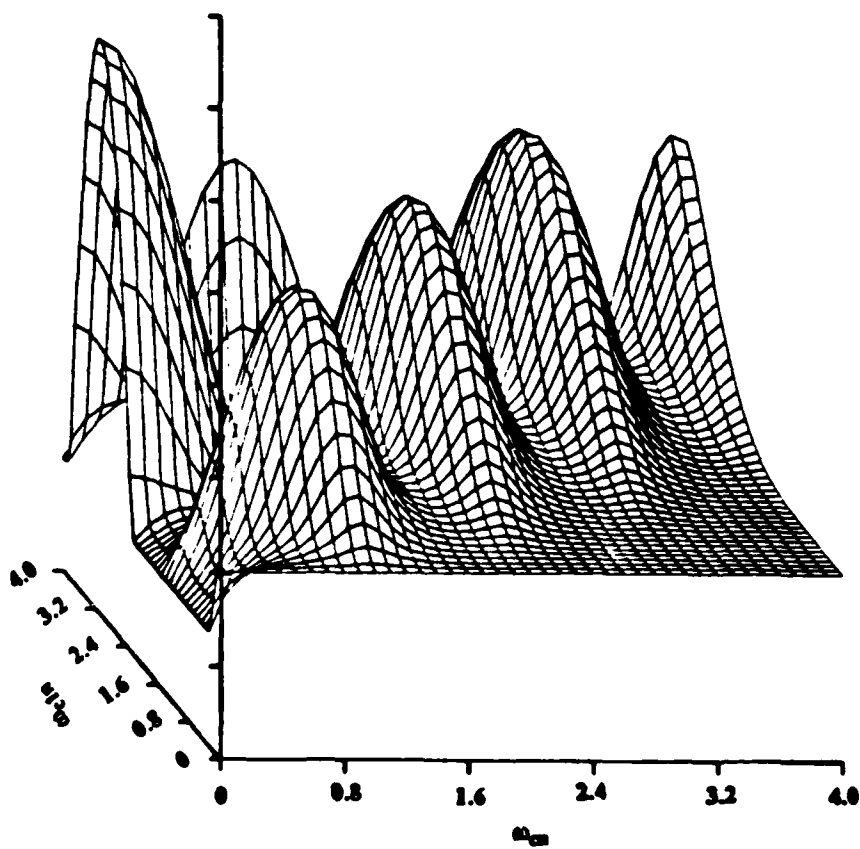
Fig. 15. Magnitude of the eigenvalues as a function of $\omega_{cn} = \omega_c/\omega$ and $\omega_{c1n} = \omega_{c1}/\omega$ for $\nu_n = 2\pi\nu/\omega = 5$. Each division on the vertical axis equals 0.2 unit.
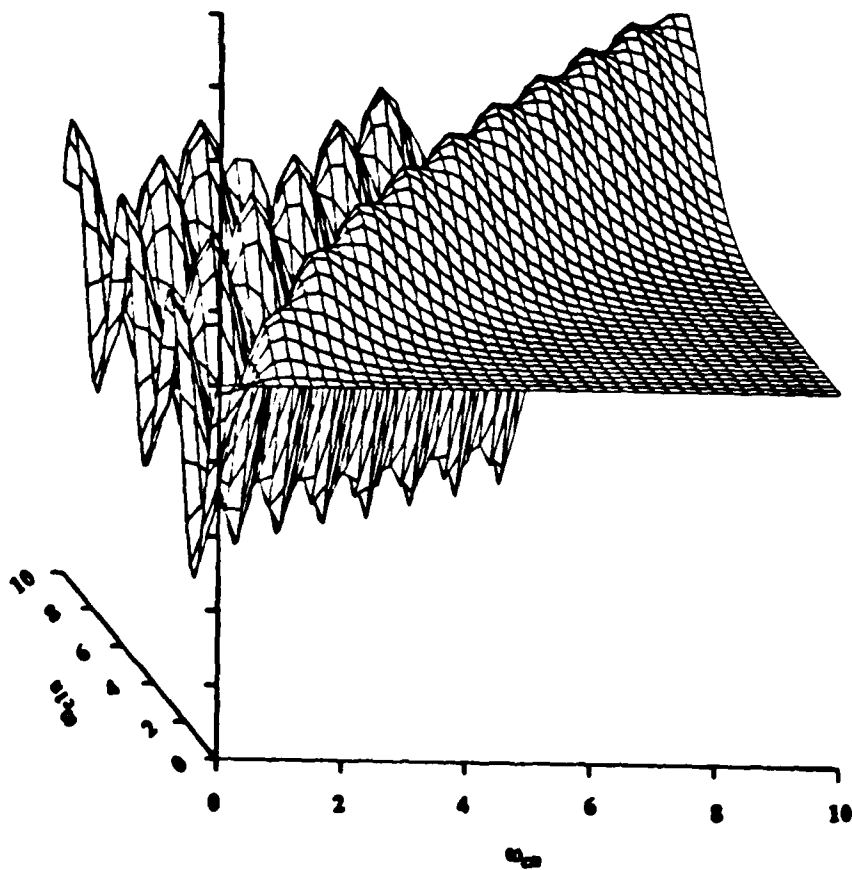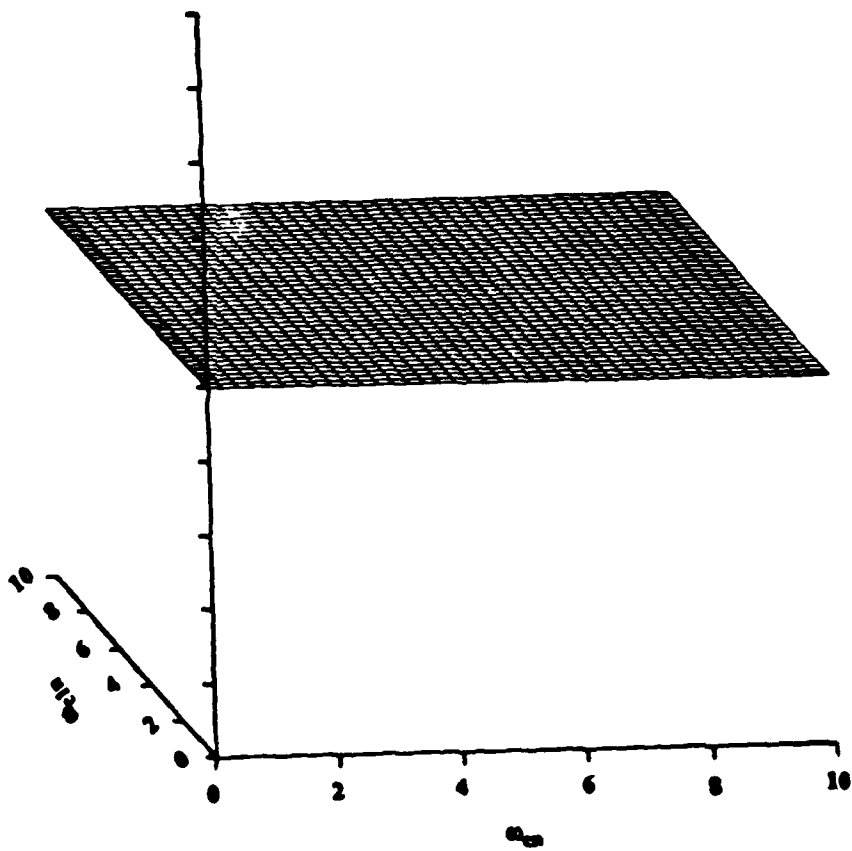
Fig. 16. Magnitude of the eigenvalues as a function of $\omega_{cn} = \omega_c/\omega$ and $\omega_{c1n} = \omega_{c1}/\omega$ for $\nu_n = 2\pi\nu/\omega = 100$. Each division on the vertical axis equals 0.2 unit.

25

Fig. 17. Magnitude of the eigenvalues as a function of $\omega_{cn} = \omega_c/\omega$ and $\omega_{c1n} = \omega_{c1}/\omega$ for $v_n = 2\pi v/\omega = 0$. This contour plot is like looking down from the top in Fig. 12. Only contour lines for eigenvalues greater than or equal to unity are shown.
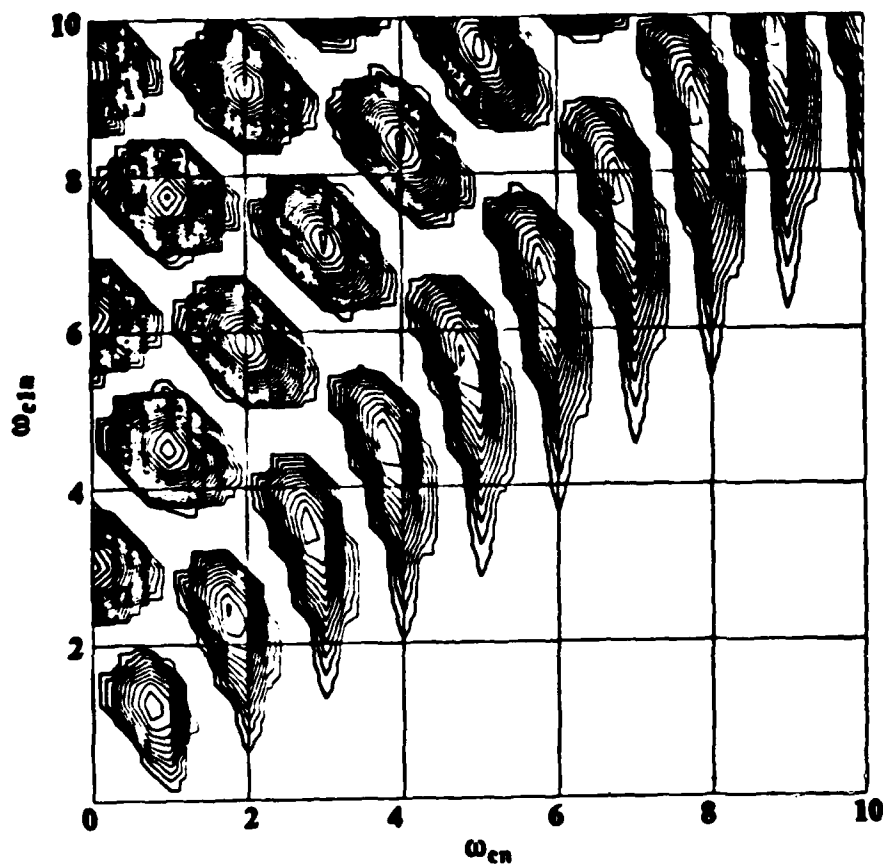
26

Fig. 18. Magnitude of the eigenvalues as a function of $\omega_{cn} = \omega_c/\omega$ and $\omega_{c1n} = \omega_{c1}/\omega$ for $v_n = 2\pi v/\omega = 1$. This contour plot is like looking down from the top in Fig. 13. Only contour lines for eigenvalues greater than or equal to unity are shown.
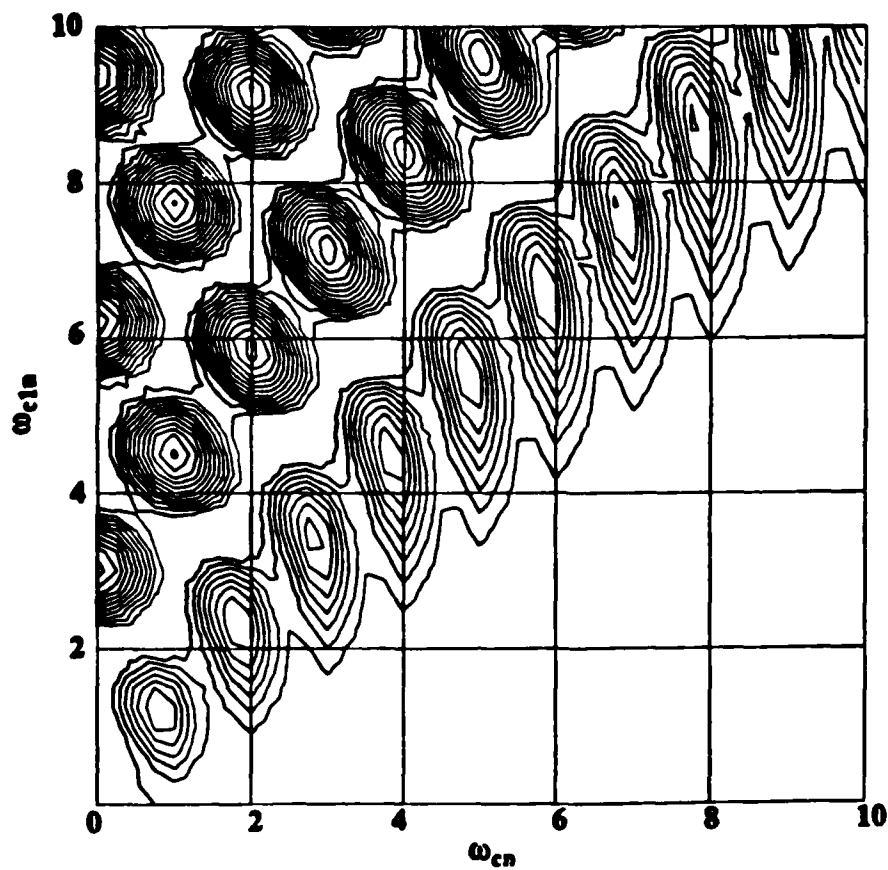
In this section, the three prominent features of the resonance response described above are explained in terms of physical concepts.

The first important concept about the interaction between the fields and the charge is that the magnetic fields do not impart any energy to the charged particle. This can be shown in the standard way by taking **v •** with both sides of (3). Only the electric field transfers energy to the charge. The magnetic fields do have a significant effect, though, because they bend the path of the particle around the magnetic field lines. This bending occurs through the **v ×B** force term, in which the force is always perpendicular to both the velocity and the magnetic field. Thus when the particle begins at rest in the presence of an **E** and **B** field, the **E** field starts it moving, and as soon as it has acquired some velocity, the **B** field begins to bend it around. The particle then moves in a sort of curved path that tends to bring it back around to the vicinity of its beginning place, similar to the paths shown in Figs. 4 and 5. How long it takes the particle to make one "revolution" (loosely speaking) depends on the magnetic field strength and the velocity.

A second important concept about the physical mechanism of interaction is that the **E** field imparts energy to the particle when **v** and **E** have a component in the same direction, and the **E** field takes energy from the particle when **v** and **E** have a component in the opposite direction. With these two concepts, the resonance response can be thought of in terms of the synchronization of the particle with **E**. The particle, intially at rest, begins to move in the direction of **E**. Since **E** is a time periodic field, after some period of time, the direction of **E** reverses. If, when **E** reverses, that reversal makes **E** and **v** in opposite directions, **E** will begin to slow the particle down. But if the magnetic field has bent the path of the particle in just the right way so that when **E** reverses direction, the velocity of the particle is still in the direction of **E**, then **E** will continue to give energy to the particle and speed it up. Fig. 4 shows just that situation. The magnetic field strength is exactly right to make the particle get around to the other side of its orbit at just the right time for its velocity to be in the same direction as **E**. Thus the **B** field can be thought of as synchronizing the position of the particle so that its velocity is in the same direction as **E** as much of the time as possible. If the magnitude of **B** is such that synchronization occurs, maximum energy is imparted to the particle, and its velocity increases rapidly. If the magnitude of **B** is such that synchronization does not occur, in the sense that the velocity of the particle is not in the same direction as **E** much of the time, relatively less energy is imparted to the particle, and its velocity does not increase much. Thus synchronization results in resonance.

The idea of synchronization explains the three prominent features of the response described in the previous section. First, the position of the peaks in Figs.17 and 18 are not drastically affected by v because the basic synchronization is not affected much by v. The damping represented by v takes energy from the particle and thus slows it, but the magnetic field still provides synchronization because the particle still gets around to the other side of its orbit at the right time to be in synchronization with **E**, but the radius of the orbit is smaller because the velocity is lower. Thus the basic mechanism

28

depends mostly on the synchronization, which is not strongly affected by the damping. If v is too high, of course, the energy extracted from the particle will be so great that its velocity will not build up, even if synchronization occurs, and no resonance will occur, as indicated by Fig. 16.

The concept of synchronization also explains why the linewidth is not zero when v is zero, as indicated by Fig. 12. The linewidth depends mainly on the synchronization. When the synchronization is very high, the velocity will build up very rapidly, corresponding to a peak in Fig. 17. When there is some synchronization, but less than that possible, the velocity will still build up, but not as rapidly, corresponding to points near, but not at, a peak in Fig. 17.

The concept of synchronization also explains why resonance occurs with an ac magnetic field present, but no dc magnetic field. The ac magnetic field has the same effect as the dc field in bending the particle's path and synchronizing it with the electric field, but in a more complicated way because the direction of the magnetic field is also reversing periodically. Thus resonance occurs because of the synchronization of v with E by the ac magnetic field, even when no dc magnetic field is present.

Finally, the idea of synchronization explains the "amplitude window," which is an element of all the above explanations. The amplitude window occurs because synchronization occurs at a given frequency only for certain combinations of dc and ac magnetic field strength. The requirement of a certain value of ac magnetic field strength for synchronization to occur, and therefore resonance to occur, is equivalent to the amplitude window.

2.6 Summary and Conclusions About Modeling

The examples given in this report show calculated trajectories for only a few of the possible combinations of parameters for which calculations could be made, but they indicate how strong resonance effects can be, and what the nature of the basic response to combinations of ac and dc magnetic fields and ac electric fields is. The eigenvalue calculations clearly define the conditions necessary for resonance to occur.

The sensitivity of the response to the values of ω, ω_c, and ω_{c1} is striking. The displacement of the particle from its initial resting position after a given number of cycles of the ac frequency can differ by orders of magnitude with the values of ω, ω_c, and ω_{c1}. This dependence of the response on the resonant conditions leads to four main conclusions from this model that are important in biological effects:

1. "Frequency windows" exist. That is, for fixed values of the other parameters, strong response will be expected only for certain values of frequency.

2. "Amplitude windows" exist. That is, for fixed values of the other parameters, strong response will be expected only for certain values of ac magnetic field strength (ω_{c1}).

3. When excitation is primarily due to an electric field alone, net charge transport will not occur.

29

When magnetic fields are present, net charge transport can occur.

4. The resonance response is strongly affected by viscous damping. Any biological effect attributed to these resonance effects would be expected to occur only in places where the effective damping is low, that is v is smaller than ω.

The prominent features of the resonant response predicted by this model have been explained in terms of the magnetic field synchronizing the particle's velocity with the electric field so that maximum energy is transferred from the electric field to the particle. Numerical values for combinations of dc magnetic field strength, ac magnetic field strength, and frequency that produce resonance for this model are given in the plots of Figs. 17 and 18.

This model provides a basic physical explanation that could apply to some of the experimental observations that have been reported in the literature (see Section 1). The model does not represent any specific biological system; it is much too simple for that. The physical explanations derived from the model might, however, be important to further understanding of resonance phenomena in biological systems that result from the application of magnetic fields. For example, periodic endogenous fields produced by an array of molecules would be expected to cause additional resonance characteristics superimposed on the synchronization effects described above. Careful experimentation will be required to pinpoint the site of the resonance response in biological systems and relate it to fundamental physical principles. Calculations for this simple physical model could serve as a first step in that process, since it provides a possible physical explanation for the so-called amplitude window.

3. EXPERIMENTAL WORK
3.1 Rationale

The experimental observations described in the literature (see Section 1) are for resonant responses in biological systems. Because of the complexity of these biological systems, identifying the site of the basic interaction may prove to be very difficult. We have taken the approach, therefore, of beginning with the simplest, stablest system that might exhibit resonance response, and then proceeding systematically to more complex systems. Accordingly, we began with a simple planar phospholipid bilayer membrane preparation, as described below. After we obtain data for that system and find out whether it shows a resonance response, we will extend the measurements to modified membranes that include for example, channels. If we do not observe resonance response, we might be able to conclude that the preparation upon which the measurements were made does not contain the elements that are responding in the biological systems. This should be important in further identifying the basic sites of interaction in biological systems.

3.2 Phospholipid Membrane Preparation

The system being used is a bilayer lipid membrane (BLM) in which a bilayer of lipid is formed across a small hole (<1 mm diameter) in a sheet of plastic separating two compartments of aqueous solution. This setup allows electrical measurements across a single membrane, and for materials to be added individually to the solutions on either side of the membrane [Finkelstein, 1974; Mountz et al, 1978].

3.2.1 Methods. The BLM is formed by the paint-brush technique. Lipid in n-decane (50 mg/ml) is brushed over the hole, separating solutions of 150 mM KCl (or NaCl) and 1mM $CaCl_2$. Directly after painting the lipid-decane mixture across the hole, there is a period of "thinning" (about 45 min) in which decane and excess lipid diffuse out of the mid portion of the membrane to the surrounding annulus, leaving a thin (6nm) bimolecular leaflet (the BLM) across the aperture. Once formed, BLMs made by this method are stable for 6-24 hours at transmembrane voltages of <250 mV.

3.2.2 Lipid Characteristics. The lipid system used (Asolectin) is derived from plant membranes and is composed of a mixture of phospholipids, predominately phosphatidylcholine, phosphatidylserine, and phosphatidylethanolamine with smaller amounts of phosphatidylinositol and phosphatidic acid. The fluidity of the acyl chain region of these lipids at room temperature (the temperature for these experiments) is comparable to biological membranes under physiological conditions. The high percentage of negatively charged phospholipids in the mixture gives the membrane an overall negative surface potential. Negative lipids have typically been found necessary for full activity of membrane proteins and interactions with cations [Brotherus et al, 1980; Wojtczak and Nalecz, 1979]. Cations, especially divalent cations (Ca^{+2}), regulate many properties of negatively charged membranes (thickness, fluidity) [Leventis et al, 1986] and their attraction for the negative charges draws them near to the membranes, increasing their concentration at the membrane surface where they may interact with proteins or channels.

Although this is a model system, conditions have been chosen to mimic physiologically relevant systems (buffer composition, lipid mixture). Asolectin has been found to be an excellent lipid mixture for reconstituting membrane proteins [Labarca, et al, 1984]. It has approximately the correct surface charge, acyl chain mobility, and bilayer thickness.

In the initial experiments, the conductance of ions (K^+, Na^+, and Ca^{+2}) across the lipid bilayer, and changes in Ca^{+2} binding to phospholipid headgroups (affecting membrane thickness and thus capacitance) will be measured. The next step will be the addition of valinomycin, a protein that shuttles K^+ across membranes, to note the effect of ion interactions with a membrane protein ion shuttle. Finally, ion channels will be incorporated into the BLMs to note changes in ion conductance through a protein channel.

3.3 Apparatus

3.3.1 Magnetic Field Coils. We designed two pairs of Helmholtz coils to produce orthogonal components of magnetic field. Each coil consists of enameled wire wound on a form with a diameter

31

of 2.5 cm. The coils of each pair are separated by 4 cm. One pair of coils is placed so as to produce a vertical component of dc magnetic field that cancels the earth's vertical component of magnetic field. The other pair is aligned with the horizontal component of the earth's magnetic field so as to produce a net dc magnetic field of the desired strength. An ac current to produce a horizontal ac magnetic field is superimposed on the dc current. The phospholipid membrane is placed appropriately in between the two pairs of coils, with the magnetic field components oriented as desired with respect to the membrane. Since the superimposing of the ac and dc currents caused some interaction of the ac and dc power supplies, in retrospect we believe it might have been better to use separate sets of coils for the ac and dc field components. We solved the problem, however, by designing a dc amplier that isolated the two sets of currents.

We measured the magnetic fields produced by the Helmholtz coils with two different instruments, and found the measured values to be very close to the calculated values. At first, we used a stereo amplifier purchased from an electronics supply house to amplify the ac current produced by a signal generator as a means of generating desired values of ac magnetic field. We found, however, that the frequency response of the stereo amplifier at the low frequencies was not good enough, and it produced strong harmonics that we could not eliminate. So we replaced the stereo amplifier by a dc amplifier of our own design; that solved the problem.

The most difficult instrumentation problem that we faced was how to eliminate the voltage induced by the ac magnetic field coils in the leads to the signal analyzer that measured the electrical impedance of the membrane. After trying a number of ways either to eliminate the induced signal or to measure it and account for it adequately, we still have not completely overcome the problem, although we have reduced it to the point that we can get meaningful data. We have concluded that eliminating the induced voltages is probably impossible, and have concentrated on ways to measure the induced voltage and properly take it into account.

3.3.2 Measuring Equipment

A block diagram of the apparatus used to produce the magnetic fields and measure the electrical impedance of the phospholipid membrane is shown in Fig. 19.
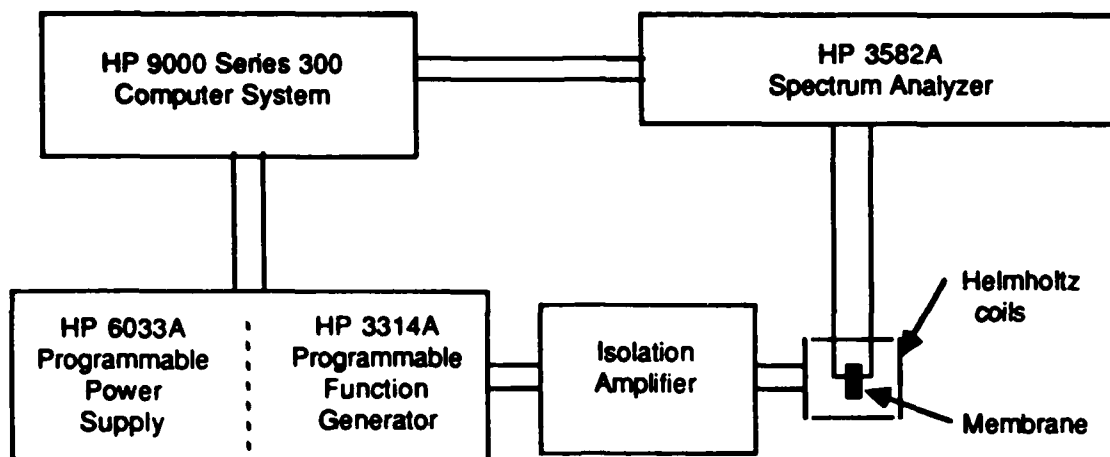
32

Fig. 19. Diagram of the system for measuring electrical impedance of phospholipid membranes exposed to combined dc and ac magnetic fields.

The computer system sets the ac magnetic field strength, the dc magnetic field strength and records the amplitude and phase of the voltage across the membrane, then resets the field strengths and repeats the process, stepping through a wide range of field strengths. Although the signal analyzer has an internal white noise source that can be used to provide the voltage for measuring the membrane impedance, we found that we got more stable and more accurate readings if we used a separate, sinusoidal generator (the HP 3310A function generator) to furnish the input voltage. Since we do not have a programmable generator for this purpose, we have had to set the frequency of the measuring voltage by hand. Also, to eliminate changes due to the voltage induced in the signal-analyzer circuit by the ac magnetic fields, we set the frequency, set the ac magnetic field strength, and step through values of the dc magnetic field strength. This makes the induced voltages constant for the entire set of readings. It also allows easy interpretation of the data, because if there is no resonance effect, all the readings will remain the same as the dc field strength is varied. Looking for a resonance effect thus amounts only to looking for changes in the voltage readings.

Measuring the impedance of the plain phospholipid membrane is difficult because the membrane looks electrically like a capacitance in parallel with a resistance. At 100 Hz, the resistance is about 10 MΩ, and the capacitance of a typical membrane is about 4,000 pF, which makes the capacitive reactance about 400 kΩ. Since the capacitive reactance is much smaller than the resistance, the capacitive reactance tends to short out the resistance and make it nearly impossible to measure. We did devise some bridge circuits to measure the capacitance and resistance separately, but found that these circuits caused too much voltage across the membrane, which destroyed it. Our membranes will rupture if more than about 250 mV is applied across them. Although there are probably ways to reduce the voltage across the membrane with the bridge circuit, we decided for now to measure the impedance directly, even though it is dominated by the capacitance. Later we plan to add valinomycin

33

to the solution in which the membrane is placed, which will lower the resistance of the membrane, and allow us to measure both its capacitance and resistance. This, of course, will be a modified membrane system, since the resistance is reduced because the valinomycin shuttles K^+ ions through the membrane, but it will be important to see if the resonant fields affect this process as well. If it seems important later, we will return to the problem of measuring the plain membrane impedance, but it seemed better now to get some experience with measuring some membranes first and see what other problems we might encounter.

4. SUMMARY AND CONCLUSIONS

We have completed the initial phases of an investigation of biological resonance reponses to combined dc-ac magnetic fields. The investigation includes both modeling and experimental work. To identify the concepts that describe resonance responses and explain the underlying physical mechanisms, we have written differential equations that describe a very simple model, one charged particle in a viscous medium exposed to a combination of dc and ac magnetic fields. Solutions to the equations explain the basic mechanisms of how frequency windows and an amplitude windows, such as those described in the literature (see Section 1), can be produced by the combined fields. The fundamental mechanism is based upon synchronization of the velocity of the particle with the electric fields to maximize transfer of energy from the electric fields to the particle. Although the model we have used is much to simple to represent an actual biological system, is does promise to provide useful information about the basic physical mechanisms that produce the resonance reponse. Features of a biological system not included in our first model would be expected to produce more complicated responses; for example, periodic endogenous fields of an array of molecules might be expected to superimpose additional resonance characteristics on the synchronization effects described in Section 2. Careful experimentation will be required to identify the site of interaction in biological systems and relate it to fundamental physical principles.

On the experimental side, we have assembled and tested apparatus for making electrical impedance measurements of planar phospholipid bilayer membranes exposed to combined dc and ac magnetic fields. The impedance is measured with a signal analyzer that is controlled by a microcomputer, which also sets the parameters such as frequency and magnetic field strength and collects and compiles the data. Preliminary data has been obtained for the plain membrane. We will soon be obtaining data for membranes with channels and other modifications.

REFERENCES

Bawin SM, Adey WR (1976): Sensitivity of calcium binding in cerebral tissue to weak environmental electric fields oscillating at low frequency. Proc Natnl Acad Sci USA 73:1999-2003.

Blackman CF, Benane SG, Rabinowitz JR, House DE, Joines WT (1985): A role for the magnetic field in the radiation-induced efflux of calcium ions from brain tissue in vitro. Bioelectromagnetics 6:327-337.

Blackman CF, Benane SC, Kinney LS, Joines WT, House DE (1982): Effects of ELF fields on calcium-ion efflux from brain tissue in vitro. Radiat Res 92:510-520.

Brotherus JR, Jost PC, Griffith, OH, Keana JF, Hokin LE (1980): Charge selectivity at the lipid-protein interface of membranous Na, K-ATPase. Proc Natnl Acad Sci USA 77:272-276.

Chiabrera A, Bianco B, Caratozzolo F, Giannetti G, Grattarola M, Viviani R (1985): Electric and magnetic field effects on ligand binding to the cell membrane. In Chiabrera A, Nicolini C, Schwan HP (eds): "Interactions Between Electromagnetic Fields and Cells."New York and London: Plenum.

Conti P, Gigante GE, Cifone MG, Alesse E, Ianni G, Reale M, Angeletti PU (1983): Reduced mitogenic stimulation of human lymphocytes by extremely low frequency electromagnetic fields. Federation of European Biochemical Societies Letters 162:156-160.

Conti P, Gigante GE, Alesse E, Cifone MG, Fieschi C, Reale M, Angeletti PU (1985): A role for Ca^{2+} in the effect of very low frequency electromagnetic field on the blastogenesis of human lymphocytes. Federation of European Biochemical Societies Letters 181:28-32.

Delgado JMR, Leal J, Monteagudo JL, Gracia MG (1982): Embryological changes induced by weak, extremely low frequency electromagnetic fields. J Anatomy 134:533-551.

Finkelstein A (1974): Bilayers: Formation, measurements, and incorporation of components. Meth Enz 32:489-501.

Jafary-Asl AH, Solanki SN, Aarholt E, Smith CW (1983): Dielectric measurements on live biological materials. J Biological Physics 11:15-22.

Labarca P, Lindstrom J, Montal M (1984): Acetylcholine receptor in planar lipid bilayers. J Gen Physiol 83:473-496.

Leventis R, Gagne J, Fuller N, Rand RP, Silvius JR (1986): Divalent cation induced fusion and lipid lateral separation in phosphatidylcholine-phosphatidic acid vesicles. Biochem 25:6978-6987.

Liboff AR (1985): Cyclotron resonance in membrane transport. In Chiabrera A, Nicolini C, Schwan HP (eds): "Interactions Between Electromagnetic Fields and Cells."New York and London: Plenum.

McLeod BR, Liboff AR (1986): Dynamic characteristics of membrane ions in multifield configurations of low-frequency electromagnetic radiation. Bioelectromagnetics 7:177-189.

Microwave News (1984): Pulsed magnetic fields: conflicting results. June, IV:1.

Mountz JD, Tien HT (1978): Bilayer lipid membranes (BLM): Study of antigen-antibody interactions. J Bioenergetics and Biomemb 10:139-151.

Reinhard H (1987): "Differential Equations, Foundations and Applications." New York: Macmillan Publishing Company.

Shampine LF, Gordon MK (1975): "Computer Solution of Ordinary Differential Equations, The Initial Value Problem." San Francisco: WH Freeman and Co.

Thomas JR, Schrot J, Liboff AR (1986): Low-intensity magnetic fields alter operant behavior in rats. Bioelectromagnetics 7:349-357.

Ubeda A, Leal J, Trillo MA, Jiminez MA, Delgado JMR (1983): Pulse shape of magnetic fields influences chick embryogenesis. J Anatomy 137:513-536.

Wojtczak L, Nalecz MJ (1979): Surface charge of biological membranes as a possible regulator of membrane-bound enzymes. Eur J Biochem 94:99-107.

DISTRIBUTION LIST

Bioelectromagnetics Program

Annual, Final and Technical Reports (one copy each except as noted)

Dr. Shirley Motzkin
Department of Biology
PINY, 333 Jay Street
Brooklyn, NY 11201

Professor Stephen Cleary
Virginia Commonwealth University
Box 694 - MCV Station
Richmond, VA 23298

Dr. Richard Frankel
MIT, Bitter National Magnet Lab
170 Albany Street
Cambridge, MA 02139

Dr. Kenneth R. Foster
Bioengineering Department
University of Pennsylvania
Philadelphia, PA 19104

Dr. William Wisecup
Bioelectromagnetics Society
P.O. Box 3729
Gaithersburg, MD 20878

Professor L. L. Van Zandt
Department of Physics
Purdue University
West Lafayette, IN 47907

Dr. Bruce Kleinstein
Information Ventures, Inc.
1500 Locust Street
Philadelphia, PA 19102

Professor Ernest Albert
Department of Anatomy
George Washington University
Washington, DC 20037

Dr. James Bond
SAI, 1710 Goodridge Drive
Post Office Box 1303
McLean, VA 22102

Professor S. M. Lindsay
Department of Physics
Arizona State University
Tempe, AZ 85287

Professor C. C. Davis
Department of Electrical Engineering
University of Maryland
College Park, MD 20742

Dr. Betty Sisken
Wenner-Gren Research Lab
University of Kentucky
Lexington, KY 40506

Mr. Henry A. Kues
Applied Physics Lab
Johns Hopkins University
Laurel, MD 20810

Professor Shiro Takashima
Bioengineering Department
University of Pennsylvania
Philadelphia, PA 19104

Professor A. W. Guy
Department of Rehab. Medicine, RJ-30
University of Washington
Seattle, WA 98195

Professor Watt W. Webb
Department of Applied Physics
Cornell University
Ithaca, NY 14853

Dr. Asher Sheppard
Research Service 151
J. L. Pettis Memorial VA Hospital
Loma Linda, CA 92357

Dr. Richard I. Magin
University of Illinois
Urbana-Champaign Campus
Urbana, IL 61801

Annual, Final and Technical Reports (one copy each except as noted)

Dr. Thomas C. Rozzell
Code 1141CB
Office of Naval Research
800 N. Quincy Street
Arlington, VA 22217-5000

Administrator   (2 copies) (Enclose DTIC Form 50)
Defense Technical Information Center
Building 5, Cameron Station
Alexandria, VA 22314

Annual and Final Reports Only (one copy each)

Life Sciences Technology
Code 125
OCNR
800 North Quincy Street
Arlington, VA 22217

Commanding Officer
Naval Medical Command
Washington, DC 20372

Commanding Officer
Naval Medical Research & Development Command
National Naval Medical Center
Bethesda, MD 20814

Commander
Chemical and Biological Sciences Division
Army Research Office, P.O. Box 12211
Research Triangle Park, NC 27709

Commander
U.S. Army Research and Development Command
Attn: SGRD-PLA
Fort Detrick
Frederick, MD 21701

Commander
USAMRIID
Fort Detrick
Frederick, MD 21701

Directorate of Life Sciences
Air Force Office of Scientific Research
Bolling Air Force Base
Washington, DC 20332

Administrative Contracting Officer
ONR Resident Representative
(address varies - obtain from Business Office)

Ms. Carol Jordan
SAI, 1710 Goodridge Drive
P.O. Box 1303
McLean, VA 22102

Professor Martin Blank
Department of Physiology
Columbia University
630 West 168th Street
New York, NY 10032

Dr. Mary Ellen O'Connor
Department of Psychology
University of Tulsa
Tulsa, OK 74104

Dr. Adrianus J. Kalmijn
Scripps Institution of Oceanography
Ocean Research Division, A-020
LaJolla, CA 92093

Professor Carl Durney
Department of Electrical Engineering
University of Utah
Salt Lake City, UT 84112

Dr. Reba Goodman
Columbia University
630 West 168th Street
New York, NY 10032

Dr. Glen Edwards
Max-Planck-Institut fur
  Festkorperforschung
Heisenbergstrasse 1
Postfach 800665
7000 Stuttgart 80
Federal Republich of Germany

Dr. Jocelyn Leal
Centro Ramon y Cajal
Departmento de Investigacion
Carretera de Colmenar, Km. 9
Madrid, SPAIN

Dr. James Lin
Bioengineering Department
University of Illinois
 at Chicago
Box 4348
Chicago, IL 60680

Dr. Robert Liburdy
Lawrence Berkeley Lab
University of California-Berkeley
Berkeley, CA 94720

Dr. E. W. Prohofsky
Purdue University
Department of Physics
Hovde Hall
West Lafayette, IN 47907

Dr. W. R. Adey
J. L. Pettis Memorial VA Hospital
11201 Benton Street
Loma Linda, CA 92357

Mr. Richard Tell
USEPA
P.O. Box 18416
Las Vegas, NV 89114

Dr. Elliot Postow
Naval Medical Research & Development
  Command
National Naval Medical Center
Bethesda, MD 20814

Dr. Edward Elson, Chief
Microwave Research
Department of Microwave Research
WRAIR
Washington, DC 20307-5100

Dr. Thomas Contreras
Navy Medical Research & Development
  Command
National Naval Medical Center
Bethesda, MD 20814

Dr. Henry Lai
Department of Pharmacology
University of Washington
Seattle, WA 98195

Dr. Raphael Lee
Department of Electrical
 Engineering & Computer Science
Massachusetts Institute of
 Technology
Cambridge, MA 02139

END

9-87

DTIC